Inorg. Chem. **1988**, *27*, 2414-2421

Contribution from the Departments of Chemistry, University of British Columbia,
Vancouver, British Columbia, Canada V6T 1Y6, and Northwestern University, Evanston, Illinois 60201

Synthesis, Characterization, and Reactivity of Bis(thioether) Complexes of (Octaethylporphyrinato)ruthenium(II)

Brian R. James,*[,1a] Andrew Pacheco,[1a] Steven J. Rettig,[1a] and James A. Ibers*[,1b]

Received March 8, 1988

Treatment of the dimer $[Ru(OEP)]_2$ (**1**, OEP = dianion of 2,3,7,8,12,13,17,18-octaethylporphyrin) with the thioethers *n*-decyl methyl sulfide (DecMS) and Ph_2S yields the low-spin complexes $Ru(OEP)L_2$, L = DecMS (**2**) and Ph_2S (**3**). Complex **2** crystallizes in the triclinic system, space group $P\bar{1}$, with $a = 9.429$ (3) Å, $b = 14.198$ (3) Å, $c = 21.392$ (5) Å, $\alpha = 87.68$ (2)°, $\beta = 79.19$ (2)°, $\gamma = 77.73$ (2)°, and $Z = 2$. Crystals of **3** are orthorhombic, space group *Pbca*, with $a = 9.569$ (1) Å, $b = 22.401$ (1) Å, $c = 23.868$ (2) Å, and $Z = 4$. The average Ru-S distance of 2.37 Å in both complexes and relatively blue-shifted α bands in the visible spectrum (in the 525-nm region) suggest little π-back-bonding in the systems. Variable-temperature ^1H NMR data reveal resolution of the protons of the axial thioether ligands (because of the porphyrin ring current), as well as the diastereotopic nature of the methylene protons of coordinated DecMS; the chirality at the coordinated sulfur atoms in **2** is *R,S* in the solid state, while in solution at ambient temperatures inversion at the sulfur is apparent, although axial ligand exchange is not observed. In contrast, **3** does undergo thioether exchange, almost certainly via a supposed five-coordinate intermediate that is also in equilibrium with **1**. Preliminary data show that **2** catalyzes autoxidation of DecMS possibly via an outer-sphere process and in situ generation of H_2O_2, while **3** is ineffective for Ph_2S oxidation because rapid decomposition to a Ru(IV) μ-oxo species occurs, probably via the five-coordinate intermediate and/or **1**.

Introduction

Interest in ruthenium porphyrin chemistry remains intense; the subject has developed largely in terms of modeling naturally occurring iron porphyrin systems,[2-9] particularly in aspects of oxidation processes of the mono-[2-4] and dioxygenase type.[5,6] As well as providing insight into heme chemistry, the chemistry of ruthenium porphyrins is maturing in its own right: novel "lower" and "higher" oxidation state species exist [Ru(0), Ru(IV), Ru(VI), and higher],[2,5-7,10,11] and unprecedented organometallic chemistry at the metal center has emerged.[11-15]

Organometallic catalysis at ruthenium porphyrins has been reported for (a) oxidation of olefins and saturated hydrocarbons,[2,5] where Ru-oxo species (formed from O_2[5,6] or an oxygen atom donor such as iodosylbenzene[2]) are probable intermediates, and (b) decarbonylation of aldehydes, which proceeds by a free-radical mechanism that, as yet, is not well-defined.[16,17] An alternative catalyzed O_2-oxidation process, not involving oxygen coordination within Ru-oxo, -peroxo, or -superoxo species, appears to operate for conversion of triphenylphosphine to its oxide;[18] the system requires acid and involves an initial one-electron outer-sphere process that generates superoxide (reactions 1 and 2). Such

$$Ru^{II}(porp)L_2 + O_2 \rightleftharpoons Ru^{III}(porp)L_2^+ + O_2^- \qquad (1)$$

$$O_2^- + H^+ \rightarrow HO_2 \rightarrow {}^1/_2(H_2O_2 + O_2) \qquad (2)$$

porp = general porphyrin dianion; L = axial ligand

reactions are now well-documented for six-coordinate porphyrin complexes of the iron subgroup, both in protein[19] and non-protein systems[8,18-22] and in other six-coordinate Ru^{II} complexes,[23] and are supported by detection of HO_2 by ESR[18,21] spectroscopy and reaction rates that are faster than dissociative loss of ligand L.[18-20,23] In the case of L = PPh_3, in the presence of excess phosphine, the peroxide generated oxidizes free PPh_3 (reaction 3), and a catalytic cycle ensues because of regeneration of Ru^{II} according to reaction 4.[18]

$$PPh_3 + H_2O_2 \rightarrow OPPh_3 + H^+ + OH^- \qquad (3)$$

$$2Ru^{III} + PPh_3 + OH^- \rightarrow 2Ru^{II} + OPPh_3 + H^+ \qquad (4)$$

More interesting substrates than tertiary phosphines are thioethers, whose selective oxidation to sulfoxides is of commercial value,[24,25] and indeed a reaction equivalent to (4) has been invoked for some Ru(non-porphyrin)-catalyzed thioether oxidations with O_2.[24b] Riley and co-workers[26,27] have also reported on Ru^{II}-(non-porphyrin)/O_2 thioether oxidation systems, but here an initial two-electron outer-sphere process to give peroxide (cf. eq 1 and

---

(1) (a) University of British Columbia (UBC). (b) Northwestern University (NW).

(2) James, B. R. In *Fundamental Research in Homogeneous Catalysis*; Shilov, A. E.; Ed.; Gordon and Breach: New York, 1986; Vol. 5, p 309, and references therein.

(3) Groves, J. T. In *Cytochrome P-450: Structure, Mechanism, and Biochemistry*; Ortiz de Montellano, P.; Ed.; Plenum: New York, 1985; Chapter I, and references therein.

(4) Ogoshi, H.; Sugimoto, H.; Yoshida, Z. *Bull. Chem. Soc. Jpn.* **1978**, *51*, 2369.

(5) Groves, J. T.; Quinn, R. *J. Am. Chem. Soc.* **1985**, *107*, 5790; *Inorg. Chem.* **1984**, *23*, 3844 and references therein.

(6) Camenzind, M. J.; James, B. R.; Dolphin, D. *J. Chem. Soc., Chem. Commun.* **1986**, 1137.

(7) Collman, J. P.; Barnes, C. E.; Brothers, P. J.; Collins, T. J.; Ozawa, T.; Gallucci, J. C.; Ibers, J. A. *J. Am. Chem. Soc.* **1984**, *106*, 5151 and references therein.

(8) James, B. R.; Dolphin, D.; Leung, T. W.; Einstein, F. W. B.; Willis, A. C. *Can. J. Chem.* **1984**, *62*, 1238 and references therein.

(9) Morishima, I.; Shiro, Y.; Takamuki, Y. *J. Am. Chem. Soc.* **1983**, *105*, 6168.

(10) Collman, J. P.; Brothers, P. J.; McElwee-White, L.; Rose, E.; Wright, L. J. *J. Am. Chem. Soc.* **1985**, *107*, 4570.

(11) Collman, J. P.; Brothers, P. J.; McElwee-White, L.; Rose, E. *J. Am. Chem. Soc.* **1985**, *107*, 6110.

(12) Sishta, C.; Ke, M.; James, B. R.; Dolphin, D. *J. Chem. Soc., Chem. Commun.* **1986**, 787.

(13) Collman, J. P.; McElwee-White, L.; Brothers, P. J.; Rose, E. *J. Am. Chem. Soc.* **1986**, *108*, 1332.

(14) Ke, M.; Rettig, S. J.; James, B. R.; Dolphin, D. *J. Chem. Soc., Chem. Commun.* **1987**, 1110.

(15) Setsune, J.-I.; Dolphin, D. *Can. J. Chem.* **1987**, *65*, 459.

(16) Domazetis, G.; James, B. R.; Tarpey, B.; Dolphin, D. *ACS Symp. Ser.* **1981**, *No. 152*, 243.

(17) Sishta, C.; Camenzind, M. J.; James, B. R.; Dolphin, D. *Inorg. Chem.* **1987**, *26*, 1181.

(18) James, B. R.; Mikkelsen, S. R.; Leung, T. W.; Williams, G. M.; Wong, R. *Inorg. Chim. Acta* **1984**, *85*, 209.

(19) Paulson, D. R.; Addison, A. W.; Dolphin, D.; James, B. R. *J. Biol. Chem.* **1979**, *254*, 7002.

(20) Chu, M. M. L.; Castro, C. E.; Hathaway, G. M. *Biochemistry* **1978**, *17*, 481.

(21) Billecke, J.; Kokisch, W.; Buchler, J. W. *J. Am. Chem. Soc.* **1980**, *102*, 3622.

(22) Buchler, J. W.; Kokisch, W. *Angew. Chem., Int. Ed. Engl.* **1981**, *20*, 403.

(23) Stanbury, D. M.; Haas, O.; Taube, H. *Inorg. Chem.* **1980**, *19*, 518.

(24) (a) Ranky, W. O.; Nelson, D. C. In *Organic Sulfur Compounds*; Kharasch, N., Ed.; Pergamon: New York, 1964; Vol. I, Chapter 17. (b) Ledlie, M. A.; Allum, K. G.; Howell, J. V.; Pitkethly, G. *J. Chem. Soc., Perkin Trans. 1* **1976**, 1734.

(25) Riley, D. P.; Correa, P. E. *J. Chem. Soc., Chem. Commun.* **1986**, 1097.

(26) Riley, D. P.; Shumate, R. S. *J. Am. Chem. Soc.* **1984**, *106*, 3179.

(27) Riley, D. P.; Oliver, J. D. *Inorg. Chem.* **1986**, *25*, 1814, 1821, 1825.

0020-1669/88/1327-2414$01.50/0 © 1988 American Chemical Society

2) is invoked, with subsequent reduction of a Ru^{IV} species by alcohol solvent back to Ru^{II} completing the catalytic cycle. Oxygen atom transfer to Me$_2$S from a Ru^{IV}–oxo complex has been demonstrated also.[28]

These various findings prompted us to initiate studies on autoxidation of thioethers using as catalysts ruthenium porphyrins, and here we report on the synthesis, characterization, and some solution chemistry of bis(thioether)(porphyrinato)ruthenium(II) complexes. The work includes crystal structure data, the first reported for ruthenium porphyrins containing axial S-bonded ligands. The complexes are of some bioinorganic interest also, in that axial S-bonded ligands are important in some iron porphyrin based enzymes[4,29] and certain electron-transfer cytochrome systems.[30]

Some preliminary findings on the Ru(OEP)(R$_2$S)$_2$[31] complexes described in the present paper were first reported at a conference.[32]

Experimental Section

Reagents, Gases, and Solvents. Spectral or reagent grade solvents were obtained from Aldrich, BDH, or Fisher Chemical Co. All solvents except for methanol (spectral grade) and deuteriated solvents were filtered through a column of activity I alumina prior to use. Where anaerobic conditions are specified, the desired solvent was degassed by three to six "freeze–pump–thaw" cycles. Thereafter, all manipulations were done under argon, by syringe and Schlenk techniques, or in vacuo, by vacuum transfer techniques.

All gases were supplied by Union Carbide of Canada Ltd. Argon was USP grade and was further purified by passing through a drying tower containing Drierite (CaSO$_4$) and a deoxygenation tower containing BASF catalyst R3-11. Carbon monoxide was CP grade and was used without further purification. Dinitrogen for the glovebox was prepurified grade.

Diphenyl sulfide (Aldrich Chemicals) was used without further purification, while decyl methyl sulfide, DecMS (Fairfield Chemicals), was filtered through activity I alumina.

Ruthenium was obtained on loan from Johnson Matthey Ltd., in the form of RuCl$_3$·3H$_2$O (~40% Ru). The free base porphyrin H$_2$(OEP) was kindly provided by Dr. D. Dolphin of this Department.

Ruthenium Complexes. Ru$_3$(CO)$_{12}$,[33] Ru(OEP)(CO)(py),[34] and Ru(OEP)(py)$_2$,[34] the necessary precursors to make [Ru(OEP)]$_2$[35] (**1**), were made by the literative procedures referenced. For all these compounds, the spectroscopic data (NMR, UV/vis, IR) were in excellent agreement with those reported previously. The air-sensitive dimer **1**, prepared by vacuum pyrolysis of Ru(OEP)(py)$_2$,[35] was stored in a dry, O$_2$-free glovebox.[36]

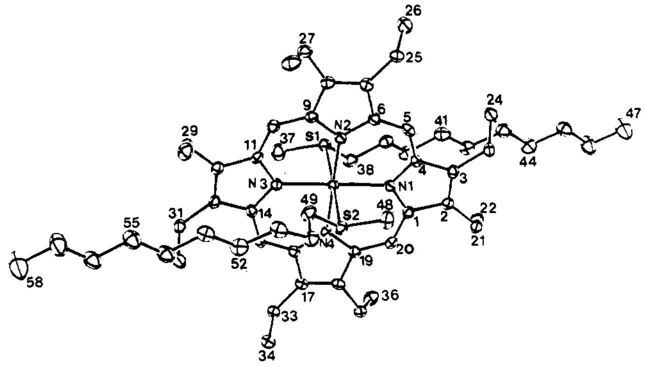

Figure 1. ORTEP drawing of the Ru(OEP)(DecMS)$_2$ structure.

Ru(OEP)(DecMS)$_2$ (2). To 75 mg (0.059 mmol) of **1** were added 67 mg (0.36 mmol) of DecMS and CH$_2$Cl$_2$ (5 mL), which immediately gave a red solution. The solvent was removed under vacuum at room temperature and the resulting oil heated to 50 °C under dynamic vacuum for 1 h to remove excess DecMS. The residual reddish purple solid was dissolved in 8 mL of *n*-pentane and the mixture filtered to remove trace Ru(OEP)(py)$_2$. To the filtrate was added 50 mL of MeOH, which formed a separate lower layer; the system was left for 20 h at room temperature and then 10 h at 5 °C, when crystals formed at the interface. These were analytically pure, even if filtered off aerobically (80% yield). Crystals suitable for an X-ray structure determination were obtained by recrystallization from 1-propanol. Anal. Calcd for C$_{58}$H$_{92}$N$_4$S$_2$Ru: C, 68.93; H, 9.18; N, 5.54. Found: C, 68.94; H, 9.19; N, 5.35. NMR (δ; C$_6$D$_6$, 20 °C): OEP, 1.99 t (CH$_3$), 3.98 q (CH$_2$), 9.70 s (H$_{meso}$); DecMS, −2.51 s (SCH$_3$), −2.46 b t (^{1}CH$_2$), −1.17 b qn (^{2}CH$_2$), −0.30 qn (^{3}CH$_2$), 0.30 qn (^{4}CH$_2$), 0.72 qn (^{5}CH$_2$), 1.00 qn (^{6}CH$_2$), 1.13 m (^{7}CH$_2$), 1.21 m (^{8}CH$_2$), 1.29 sx (^{9}CH$_2$), 0.93 t (^{10}CH$_3$). UV/vis (C$_6$H$_6$; λ_{max}, nm (log ϵ)): 525 (4.42), 498 (4.16), 408 (5.23).

Ru(OEP)(SPh$_2$)$_2$ (3). To 100 mg (0.079 mmol) of **1** were added 78 mg (0.42 mmol) of Ph$_2$S and dry CH$_2$Cl$_2$ (20 mL). The solvent was slowly removed under vacuum at room temperature while the solution was stirred, and the color changed from brownish green to bright red. After complete solvent removal (~45 min), the resulting red solid was dissolved in *n*-heptane (30 mL) and the mixture filtered to remove a trace of Ru(OEP)(py)$_2$. The solution volume was reduced by half under vacuum; the remaining solution was then refluxed until no solid was seen (~30 min) and then left overnight at room temperature. The crystals obtained (42% yield) were suitable for X-ray analysis. Anal. Calcd for C$_{60}$H$_{64}$N$_4$S$_2$Ru: C, 71.61; H, 6.41; N, 5.57. Found: C, 71.87; H, 6.53; N, 5.80. NMR (δ; C$_6$D$_6$, 20 °C): OEP, 1.93 t (CH$_3$), 3.90 q (CH$_2$), 9.50 s (H$_{meso}$); SPh$_2$, 4.04 br (H$_o$), 6.08 br (H$_m$), 6.37 br (H$_p$). UV/vis (C$_6$H$_6$; λ_{max}, nm (log ϵ)): 527 (4.28), 502 (4.07), 408 (5.38).

Instrumentation. UV/vis spectra were recorded on a Cary 17 instrument at room temperature. Data for **3** were measured in the presence of a 50-fold excess of free Ph$_2$S, when the Beer–Lambert law was obeyed; solutions of **2** gave a linear dependence of absorption vs concentration in the absence of added DecMS. Room-temperature ^{1}H NMR spectra of C$_6$D$_6$ solutions of **2** and **3** were run on a Bruker WH-400 FT machine; the peaks for **2** were assigned by using spin-decoupling or spin-tickling techniques. Variable-temperature ^{1}H NMR spectra were measured in toluene-*d*$_8$ by using a Varian XL-300 FT instrument.

Elemental analyses were carried out by P. Borda of UBC.

X-ray Crystallographic Analyses

Crystallographic data for Ru(OEP)(DecMS)$_2$ (**2**) and Ru(OEP)(SPh$_2$)$_2$ (**3**) appear in Table I. The intensities of the standard reflections showed only small random variations for both data collections. The structures were solved by conventional heavy-atom methods,[38] the coordinates of the Ru, S, and N atoms being determined from the Patterson functions and those of the remaining non-hydrogen atoms from subsequent difference maps. In the final stages of the full-matrix least-squares refinements, the non-hydrogen atoms were refined with anisotropic thermal parameters and the hydrogen atoms fixed in idealized positions [C–H = 0.95 Å, $B_H = B_{eq}(C) + 1$ Å^2 for **2**; C(sp^2)–H = 0.97 Å, C(sp^3)–H = 0.98 Å, $U_H \propto U_{eq}(C)$ for **3**]. Scattering factors and anomalous dispersion corrections (Ru, S) were taken from ref 39. Final difference maps were essentially featureless. Analysis of $\sum w\Delta^2$ over ranges of θ,

---

[28] Roecker, L.; Dobson, J. C.; Vining, W. J.; Meyer, T. J. *Inorg. Chem.* **1987**, *26*, 779.

[29] (a) English, D. R.; Hendrickson, D. N.; Suslick, K. S.; Eigenbrot, C. W., Jr.; Scheidt, W. R. *J. Am. Chem. Soc.* **1984**, *106*, 7258. (b) Scheidt, W. R.; Reed, C. A. *Chem. Rev.* **1981**, *81*, 543. (c) Mashiko, T.; Marchon, J.-C.; Musser, D. T.; Reed, C. A.; Kastner, M. E.; Scheidt, W. R. *J. Am. Chem. Soc.* **1979**, *101*, 3653. (d) Mashiko, T.; Reed, C. A.; Haller, K. J.; Kastner, M. E.; Scheidt, W. R. *J. Am. Chem. Soc.* **1981**, *103*, 5758.

[30] Koller, K. B.; Hawkridge, F. M. *J. Am. Chem. Soc.* **1985**, *107*, 7412 and references therein.

[31] Abbreviations used: OEP = dianion of 2,3,7,8,12,13,17,18-octaethylporphyrin; TPP = dianion of 5,10,15,20-tetraphenylporphyrin; R = alkyl or aryl; DecMS = *n*-decyl methyl sulfide; DMSO = dimethyl sulfoxide; py = pyridine; dpm = bis(diphenylphosphino)methane; phen = *o*-phenanthroline; Im = imidazole. For the NMR data, the following abbreviations are used: s = singlet, t = triplet, q = quartet, qn = quintet, sx = sextet, b = broad, m = multiplet.

[32] (a) James, B. R.; Pacheco, A.; Rettig, S. J.; Thorburn, I. S.; Ball, R. G.; Ibers, J. A. *Proc. 5th Int. Symp. Homogeneous Catal.* **1986**, S-13. (b) *J. Mol. Catal.* **1987**, *41*, 147.

[33] Bruce, M. I.; Matisons, J. G.; Wallis, R. C.; Patrick, J. M.; Skelton, B. W.; White, A. M. *J. Chem. Soc., Dalton Trans.* **1983**, 2365.

[34] Antipas, A.; Buchler, J. W.; Gouterman, M.; Smith, P. D. *J. Am. Chem. Soc.* **1978**, *100*, 3015.

[35] Collman, J. P.; Barnes, C. E.; Swepston, P. N.; Ibers, J. A. *J. Am. Chem. Soc.* **1984**, *106*, 3500.

[36] The N$_2$ atmosphere within the box was continuously recirculated through a Dri-Train HE-493 purification tower packed with 2.4 kg of 3-Å molecular sieves, 1.5 kg of 7-Å molecular sieves, and 2 kg of Ridox deoxygenation catalyst. This treatment kept the concentration of O$_2$ and H$_2$O below 1 ppm, as evidenced by the long lifetime of an exposed 25-W light bulb filament within the box.[37]

[37] Sekutowski, D. G.; Stucky, G. D. *J. Chem. Educ.* **1976**, *53*, 110.

[38] Programs and methods used are standard. For Ru(OEP)(DecMS)$_2$ refer to: Waters, J. M.; Ibers, J. A. *Inorg. Chem.* **1977**, *16*, 3273. For Ru(OEP)(SPh$_2$)$_2$ refer to: Lee, C.-L.; Yang, Y.-P.; Rettig, S. J.; James, B. R.; Nelson, D. A.; Lilga, M. A. *Organometallics* **1986**, *5*, 2220.

[39] *International Tables for X-ray Crystallography*; Kynoch: Birmingham, England, 1974; Vol. IV, pp 99–102, 149 (present distributor: D. Reidel, Dordrecht, The Netherlands).

Table I. Crystal Data and Data Collection Procedure for Ru(OEP)(DecMS)$_2$ (**2**) and Ru(OEP)(SPh$_2$)$_2$ (**3**)[a]

compd	Ru(OEP)(CH$_3$SC$_{10}$H$_{21}$)$_2$ (**2**)	Ru(OEP)(SPh$_2$)$_2$ (**3**)
formula	$C_{58}H_{92}N_4RuS_2$	$C_{60}H_{64}N_4RuS_2$
fw	1009.81	1006.38
space group	C_i^1–$P\bar{1}$	D_{2h}^{15}–$Pbca$
a, Å	9.429 (3)	9.569 (1)
b, Å	14.198 (3)	22.401 (1)
c, Å	21.392 (5)	23.868 (2)
α, deg	87.68 (2)	90
β, deg	79.19 (2)	90
γ, deg	77.73 (2)	90
vol, Å^3	2749	5116
Z	2	4
temp, °C	−150[b]	22
density (calcd), g/cm^3	1.221	1.307
cryst planes	{010}, [0.119];[c] {001}, [0.275]; {100}, [0.390]; ($0\bar{1}\bar{2}$), [0.126]	{111}, [0.325]; {001}, [0.256]; {010}, [0.175]; {100}, [0.325]
cryst vol, mm^3	0.013	0.013
linear abs coeff, cm^{-1}	3.89	4.19
transmission factors	0.901–0.955[d]	
detector aperture (17.3 cm from cryst)	3 mm high by 2 mm wide	4 mm high by (2 + tan θ) mm wide
takeoff angle, deg	2.5	2.7
scan mode	ω–2θ	ω–2θ
scan speed, deg/min	2 in ω for $2\theta < 30°$; 1 in ω thereafter[e]	10 in. ω, rescan time limit of 60 s
2θ limits, deg	$2 < 2\theta < 50$	$1 < 2\theta < 55$
bkg counts	$^1/_4$ of scan range on each side of rfln	
std rflns	6 in diverse regions of reciprocal space remeasd every 3 h of X-ray exposure time	3 remeasd every 1 h
scan range, deg	−0.9 below $2\theta(K\alpha_1)$ to 0.9° above $2\theta(K\alpha_2)$	0.55 + 0.35 tan θ (in ω)
data collected	$\pm h, \pm k, +l$	$+h, +k, +l$
no. of unique data	9548	5865
no. of unique data with $F_o^2 > n\sigma(F_o^2)$	7279 ($n = 3$)	2424 ($n = 2$)
p factor for $\sigma(F_0^2)$	0.03	0.04
no. of variables	586	304
$R(F)$ ($F_o^2 > n\sigma(F_o^2)$)	0.046	0.042
$R_w(F)$ ($F_0^2 > n\sigma(F_0^2)$)	0.051	0.039
$R(F^2)$	0.075[f]	
$R_w(F^2)$	0.107	
error in observn of unit wt, e^2	1.48	1.41

[a] Enraf-Nonius CAD-4 diffractometer, Mo Kα radiation (λ_{a_1} = 0.709 30 Å, λ_{α_2} = 0.713 59 Å), graphite monochromator. Structure **2** was determined at NW and **3** at UBC. [b] The low-temperature system is from a design by Prof. J. J. Bonnet and S. Askenazy and is commercially available from Soterem, Z. I. de Vic, 31320 Castanet-Tolosan, France. [c] The numbers in brackets are the distances in millimeters between parallel faces of the preceding form. For ($0\bar{1}\bar{2}$) it is the distance from the center of the crystal as defined by the other faces. [d] Analytical method used (de Meulenaer, J.; Tompa, H. *Acta Crystallogr.* **1965**, *19*, 1014). [e] Reflections having $F_o^2 < 3\sigma(F_o^2)$ were rescanned to achieve a 3σ level up to a maximum scan time of 100 s for $2\theta < 30°$; 150 s was used thereafter. [f] Final refinement on F^2, with use of all data.

F_o, and Miller indices showed no unusual trends. Standard error weights were employed in each of the crystallographic analyses.

Final positional and equivalent isotropic thermal parameters are given in Tables II and III. Selected bond lengths, bond angles, and comparisons of mean structural parameters appear in Tables IV–VI. Calculated hydrogen parameters, a complete list of bond lengths and angles, anisotropic thermal parameters, displacements of atoms from the porphyrin plane, dihedral angles between the porphyrin core and pyrrole rings, and structure amplitudes for both complexes are included as supplementary material (Tables S1–S12).

Results and Discussion

The red-purple, six-coordinate, low-spin complexes Ru(OEP)(DecMS)$_2$ (**2**) and Ru(OEP)(SPh$_2$)$_2$ (**3**) are readily obtained from the useful precursor [Ru(OEP)]$_2$[35] by treatment with excess thioether in CH$_2$Cl$_2$ at room temperature. Decyl methyl sulfide was used as a dialkyl sulfide in lieu of Me$_2$S because of the relative ease of handling the less volatile higher molecular weight homologue. The common synthetic route to Ru(OEP)L$_2$ complexes via photolysis of the Ru(OEP)(CO) precursor in the presence of L[34] gave lower yields with L = R$_2$S, and it proved difficult to separate unreacted thioether from the product.

Solid-State Structures of 2 and 3. The crystal structures of Ru(OEP)L$_2$ with L = DecMS (**2**) and Ph$_2$S (**3**) are the first reported for ruthenium porphyrin complexes containing S-bound axial ligands. Indeed, outside of in situ addition of alkanethiolates (–SR) to Ru(OEP)(CO) (used as a model for the carbonyl adduct of reduced cytochrome P-450),[4] isolation of Ru(OEP)(DMSO)$_2$,[40a] and isolation of DMSO complexes of (phthalocyaninato)ruthenium(II), a tetraaza porphyrin in which DMSO is probably S-bonded,[40b] we are unaware of any other reports on the interaction of S-containing compounds with ruthenium porphyrins.

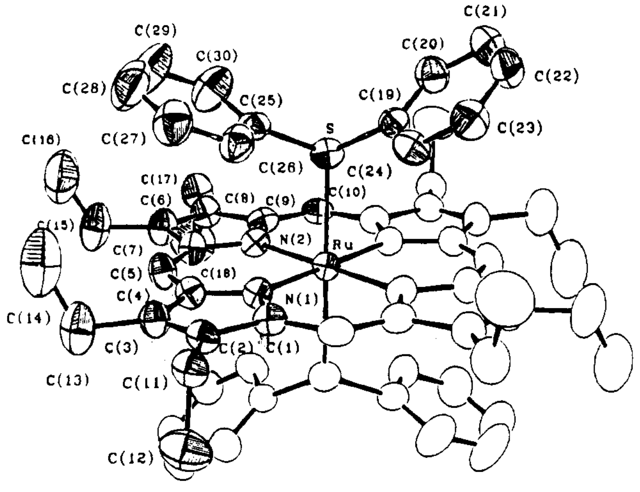

Figure 2. ORTEP drawing of the Ru(OEP)(SPh$_2$)$_2$ structure. The complex is centrosymmetric.

In both structures **2** and **3** (Figures 1 and 2), the Ru is essentially in the porphyrin plane, which itself is little distorted. The S–Ru–S axes are close to being orthogonal to the porphyrin plane, the distortions being somewhat greater in **3**; similar distortions are found in other Ru(porp)L$_2$ complexes, where L is a large axial

---

(40) (a) Hopf, F. R.; O'Brien, T. P.; Scheidt, W. R.; Whitten, D. G. *J. Am. Chem. Soc.* **1975**, *97*, 277. (b) Dolphin, D.; James, B. R.; Murray, A. J.; Thornback, J. R. *Can. J. Chem.* **1980**, *58*, 1125.

Table II. Final Positions (Fractional ×10^4, Ru and S ×10^5) and Isotropic Thermal Parameters (B_{eq}) for Ru(OEP)(DecMS)$_2$[a]

atom	x	y	z	B_{eq}, Å^2
Ru	2517 (3)	224 (2)	24136 (1)	1.344 (7)
S(1)	19077 (9)	−5122 (6)	14541 (4)	1.72 (2)
S(2)	−14087 (9)	6003 (6)	33532 (4)	1.82 (2)
N(1)	−1007 (3)	−937 (2)	2285 (1)	1.49 (7)
N(2)	1549 (3)	−1020 (2)	2865 (1)	1.57 (7)
N(3)	1497 (3)	990 (2)	2562 (1)	1.53 (7)
N(4)	−1064 (3)	1068 (2)	1975 (1)	1.50 (7)
C(1)	−2260 (4)	−745 (2)	2024 (2)	1.55 (9)
C(2)	−2861 (4)	−1613 (2)	2036 (2)	1.55 (9)
C(3)	−1958 (4)	−2319 (2)	2304 (2)	1.65 (9)
C(4)	−807 (4)	−1886 (2)	2470 (2)	1.58 (9)
C(5)	315 (4)	−2348 (2)	2789 (2)	1.8 (1)
C(6)	1394 (4)	−1961 (2)	2975 (2)	1.68 (9)
C(7)	2556 (4)	−2471 (2)	3297 (2)	1.72 (9)
C(8)	3440 (4)	−1850 (3)	3355 (2)	1.8 (1)
C(9)	2797 (4)	−935 (2)	3088 (2)	1.52 (9)
C(10)	3341 (4)	−98 (3)	3061 (2)	1.8 (1)
C(11)	2732 (4)	799 (2)	2835 (2)	1.53 (9)
C(12)	3252 (4)	1679 (2)	2878 (2)	1.65 (9)
C(13)	2296 (4)	2396 (2)	2636 (2)	1.65 (9)
C(14)	1216 (4)	1955 (2)	2426 (2)	1.58 (9)
C(15)	85 (4)	2416 (2)	2122 (2)	1.55 (9)
C(16)	−969 (4)	2022 (2)	1908 (2)	1.50 (9)
C(17)	−2173 (4)	2549 (2)	1616 (2)	1.68 (9)
C(18)	−2999 (4)	1915 (2)	1526 (2)	1.65 (9)
C(19)	−2314 (4)	989 (2)	1759 (2)	1.57 (9)
C(20)	−2858 (4)	148 (3)	1785 (2)	1.61 (9)
C(21)	−4241 (4)	−1664 (3)	1793 (2)	1.8 (1)
C(22)	−4011 (4)	−1748 (3)	1071 (2)	2.3 (1)
C(23)	−2041 (4)	−3355 (2)	2421 (2)	1.8 (1)
C(24)	−906 (4)	−4048 (3)	1953 (2)	2.5 (1)
C(25)	2743 (4)	−3512 (3)	3500 (2)	2.1 (1)
C(26)	3625 (5)	−4196 (3)	2978 (2)	3.0 (1)
C(27)	4826 (4)	−2034 (3)	3632 (2)	2.0 (1)
C(28)	4593 (4)	−1641 (3)	4305 (2)	2.8 (1)
C(29)	4570 (4)	1744 (3)	3161 (2)	2.0 (1)
C(30)	4244 (4)	1779 (3)	3887 (2)	2.6 (1)
C(31)	2272 (4)	3457 (3)	2604 (2)	1.9 (1)
C(32)	1112 (5)	4021 (3)	3127 (2)	2.7 (1)
C(33)	−2449 (4)	3610 (2)	1485 (2)	1.9 (1)
C(34)	−3342 (4)	4195 (3)	2064 (2)	2.5 (1)
C(35)	−4394 (4)	2099 (3)	1251 (2)	1.9 (1)
C(36)	−4162 (4)	1739 (3)	572 (2)	2.5 (1)
C(37)	2759 (5)	482 (3)	1141 (2)	2.8 (1)
C(38)	912 (4)	−604 (3)	813 (2)	2.2 (1)
C(39)	736 (4)	−1620 (3)	749 (2)	2.2 (1)
C(40)	−51 (4)	−1742 (3)	204 (2)	2.3 (1)
C(41)	−224 (4)	−2770 (3)	153 (2)	2.5 (1)
C(42)	−1228 (4)	−2924 (3)	−293 (2)	2.2 (1)
C(43)	−1476 (4)	−3951 (3)	−271 (2)	2.6 (1)
C(44)	−2574 (5)	−4102 (3)	−672 (2)	2.9 (1)
C(45)	−2835 (5)	−5118 (3)	−675 (2)	2.8 (1)
C(46)	−3945 (6)	−5243 (3)	−1070 (2)	3.8 (1)
C(47)	−4211 (6)	−6244 (4)	−1091 (3)	4.6 (2)
C(48)	−2211 (5)	−369 (3)	3727 (2)	2.6 (1)
C(49)	−342 (4)	818 (3)	3933 (2)	2.3 (1)
C(50)	−1271 (4)	1157 (3)	4561 (2)	2.5 (1)
C(51)	−361 (4)	1477 (3)	5015 (2)	2.5 (1)
C(52)	−26 (5)	2469 (3)	4871 (2)	2.7 (1)
C(53)	998 (4)	2721 (3)	5286 (2)	2.4 (1)
C(54)	1236 (5)	3747 (3)	5204 (2)	2.8 (1)
C(55)	2303 (5)	3969 (3)	5595 (2)	3.2 (1)
C(56)	2520 (5)	4997 (3)	5563 (2)	3.1 (1)
C(57)	3583 (6)	5184 (3)	5964 (3)	4.3 (2)
C(58)	3799 (7)	6201 (4)	5956 (3)	5.7 (2)

[a] Standard deviations in parentheses.

Table III. Final Positional (Fractional ×10^4, Ru and S ×10^5) and Isotropic Thermal Parameters (U_{eq}, ×10^3 Å^2) for Ru(OEP)(SPh$_2$)$_2$[a]

atom	x	y	z	U_{eq}
Ru	50000	50000	50000	32
S	27385 (13)	45980 (5)	48509 (5)	40
N(1)	6109 (4)	4302 (1)	4667 (2)	33
N(2)	4735 (4)	5354 (1)	4216 (1)	35
C(1)	6696 (5)	3836 (2)	4959 (2)	38
C(2)	7432 (5)	3446 (2)	4569 (2)	39
C(3)	7298 (6)	3690 (2)	4051 (2)	45
C(4)	6464 (6)	4228 (2)	4113 (2)	40
C(5)	6058 (6)	4610 (2)	3686 (2)	45
C(6)	5262 (5)	5124 (2)	3724 (2)	42
C(7)	4838 (6)	5503 (2)	3260 (2)	50
C(8)	4097 (6)	5960 (2)	3477 (2)	45
C(9)	4029 (5)	5867 (2)	4081 (2)	38
C(10)	3373 (5)	6239 (2)	4465 (2)	38
C(11)	8186 (5)	2877 (2)	4717 (2)	44
C(12)	9724 (6)	2964 (3)	4834 (3)	74
C(13)	7987 (7)	3468 (3)	3506 (3)	70
C(14)	6863 (10)	3137 (3)	3168 (3)	115
C(15)	5228 (7)	5396 (2)	2653 (2)	72
C(16)	4450 (9)	4892 (3)	2398 (3)	112
C(17)	3487 (7)	6489 (3)	3166 (2)	59
C(18)	4552 (8)	6979 (3)	3098 (3)	90
C(19)	1974 (5)	4227 (2)	5443 (2)	41
C(20)	689 (6)	4419 (2)	5611 (2)	53
C(21)	24 (7)	4156 (3)	6071 (2)	69
C(22)	678 (7)	3709 (3)	6355 (2)	60
C(23)	1978 (7)	3529 (3)	6200 (2)	57
C(24)	2642 (6)	3782 (2)	5742 (2)	47
C(25)	2780 (6)	4025 (2)	4324 (2)	43
C(26)	3469 (7)	3490 (3)	4394 (2)	54
C(27)	3519 (7)	3087 (2)	3955 (3)	69
C(28)	2894 (9)	3219 (4)	3462 (3)	92
C(29)	2209 (9)	3747 (4)	3394 (3)	101
C(30)	2120 (8)	4162 (3)	3829 (3)	80

[a] Standard deviations in parentheses.

Table IV. Selected Bond Distances (Å) and Bond Angles (deg) in Ru(OEP)(DecMS)$_2$[a]

	Distances[b]		
Ru–S(1)	2.376 (1)	Ru–N(2)	2.044 (3)
Ru–S(2)	2.361 (1)	Ru–N(3)	2.056 (3)
Ru–N(1)	2.044 (3)	Ru–N(4)	2.041 (3)
	Angles[c]		
N(1)–Ru–S(1)	90.2 (1)	S(1)–Ru–S(2)	178.27 (3)
N(2)–Ru–S(1)	86.9 (1)	Ru–S(1)–C(37)	107.5 (1)
N(3)–Ru–S(1)	90.9 (1)	Ru–S(1)–C(38)	111.2 (1)
N(4)–Ru–S(1)	94.0 (1)	Ru–S(2)–C(48)	109.0 (1)
N(1)–Ru–S(2)	90.7 (1)	Ru–S(2)–C(49)	108.1 (1)
N(2)–Ru–S(2)	94.7 (1)	C(37)–S(1)–C(38)	98.4 (2)
N(3)–Ru–S(2)	88.3 (1)	C(48)–S(2)–C(49)	101.0 (2)
N(4)–Ru–S(2)	84.5 (1)		

[a] Standard deviations in parentheses. [b] The S–C bond distances vary from 1.797 (4) to 1.825 (4) Å. [c] N–Ru–N angles are close to 90° (within 0.3°) or 180° (within 1.1°).

Table V. Selected Bond Distances (Å) and Bond Angles (deg) in Ru(OEP)(SPh$_2$)$_2$[a]

	Distances		
Ru–S	2.371 (1)	S–C(19)	1.796 (5)
Ru–N(1)	2.050 (3)	S–C(25)	1.798 (5)
Ru–N(2)	2.048 (3)		
	Angles		
S–Ru–N(1)	97.2 (1)	N(1)–Ru–S′	82.8 (1)
S–Ru–N(2)	84.1 (1)	N(1)–Ru–N(2)′	89.7 (1)
S–Ru–N(1)′	82.8 (1)	Ru–S–C(19)	115.4 (2)
S–Ru–N(2)′	95.9 (1)	Ru–S–C(25)	110.9 (2)
N(1)–Ru–N(2)	90.3 (1)	C(19)–S–C(25)	103.3 (2)

[a] Standard deviations in parentheses.

ligand, e.g. a tertiary phosphine,[41] and probably result from crystal packing. Complex **3** has a crystallographic inversion center, and while **2** appears to have such a center, a number of unsuccessful attempts were made to find it. The cell did not transform to a higher symmetry, and a listing of F_o as a function of 2θ did not reveal duplicate data collection; further, the lattice produced by

---

[41] (a) Ball, R. G.; Domazetis, G.; Dolphin, D.; James, B. R.; Trotter, J. *Inorg. Chem.* **1981**, *20*, 1556. (b) Ariel, S.; Dolphin, D.; Domazetis, G.; James, B. R.; Leung, T. W.; Rettig, S. J.; Trotter, J.; Williams, G. M. *Can. J. Chem.* **1984**, *62*, 755.

Table VI. Averaged Bond Lengths (Å) and Angles (deg) for the Porphyrin Core of Ruthenium Porphyrin Complexes

length or angle	Ru(TPP)-(CO)(py)$^{a\ 56}$	Ru(TPP)-(CO)(EtOH)$^{a\ 57}$	Ru(TPP)-(OEt)(EtOH)$^{b\ 7}$	Ru(TPP)-(dpm)$_2{}^{a\ 41a}$	Ru(OEP)-(PPh$_3$)$_2{}^{a\ 41b}$	Ru(OEP)-(Br)(PPh$_3$)$^{a\ 8}$	Ru(OEP)-(DecMS)$_2{}^{c}$ (this work)	Ru(OEP)-(SPh$_2$)$_2{}^{a}$ (this work)
Ru–N	2.052 (9)^d	2.049 (5)	2.040 (6)	2.041 (8)	2.051 (5)	2.034 (11)	2.046 (6)	2.049 (3)
N–$C_a{}^e$	1.370 (9)	1.374 (8)	1.377 (5)	1.38 (2)	1.374 (5)	1.39 (3)	1.374 (4)	1.375 (5)
C_a–C_m	1.395 (10)	1.393 (10)	1.398 (5)	1.39 (2)	1.386 (10)	1.36 (3)	1.389 (5)	1.386 (6)
C_a–C_b	1.446 (11)	1.437 (13)	1.437 (5)	1.43 (2)	1.453 (6)	1.45 (2)	1.453 (5)	1.456 (6)
C_b–C_b	1.333 (11)	1.327 (12)	1.350 (6)	1.32 (2)	1.354 (8)	1.37 (2)	1.357 (6)	1.354 (6)
C_a–N–C_a	107.8 (6)	107.4 (6)	106.6 (3)	106.5 (2)	106.8 (5)	107 (2)	106.7 (3)	107.1 (4)
N–C_a–C_b	108.3 (8)	108.3 (6)	109.3 (3)	108 (1)	109.6 (3)	109 (2)	109.7 (3)	109.3 (4)
N–C_a–C_m	126.4 (7)	125.6 (6)	125.6 (4)	125 (1)	123.9 (4)	124 (3)	124.5 (3)	124.7 (4)
C_a–C_b–C_b	107.8 (8)	108.0 (8)	107.4 (4)	108 (1)	107.1 (4)	107 (2)	107.0 (3)	107.1 (4)
C_a–C_m–C_a	125.0 (7)	126.1 (6)	125.6 (4)	126 (1)	129.1 (4)	130 (6)	127.9 (4)	127.7 (8)

[a] Data collected at room temperature. [b] Data collected at −160 °C. [c] Data collected at −150 °C. [d] Error in the mean value is the larger of the unweighted estimated standard deviation of a single observation or the error estimated from the least-squares inverse matrix. [e] Labeling: C_a and C_b refer to carbon atoms α and β to the pyrrole N, respectively; C_m refers to the meso carbon atoms.

the Ru positions only did not suggest higher symmetry.

The Ru–S bond distances average 2.37 Å, exactly the sum of the covalent radii for Ru and S.[42] A survey of the literature for complexes containing Ru–S bonds within organosulfur moieties[27,43-55] shows lengths varying from 2.188 Å in Ru(NH$_3$)$_5$(DMSO)$^{2+}$[43] to 2.45 Å in a S-bound thiobenzoate in *cis,cis,cis*-Ru(SOCPh)$_2$(phen)(PMe$_2$Ph)$_2$.[49] The shorter bonds have generally been attributed to the presence of S → Ru π-back-bonding, this being greater when the S ligand is trans to a σ-donor/non-π-acceptor, and weaker when trans to another π-acceptor (including mutually trans S ligands);[43-55] this generalization is particularly well documented for sulfoxide S-liganded systems.[43-46] For the reported thioether-liganded systems,[27,47,50] including our porphyrin data, complexes with trans thioether ligands have Ru–S bond lengths in the range 2.361–2.393 Å, while in species where there is no S-bonded ligands or a π-back-bonding ligand trans to the thioether, the Ru–S bond lengths are in the range 2.323–2.351 Å. The limited data suggest that thioethers are capable of a small degree (relative to that, for example, of sulfoxides) of π-back-bonding.

In the ruthenium thioether and sulfoxide systems mentioned above,[27,43-48,50] and in **2** and **3** (and in η^1, S-bonded thiophene derivatives[54,55]), the S atom is always pyramidal. In the thioether (and sulfoxide) complexes, the C–S–C and Ru–S–C bond angles range from 92.3 to 103.3° and from 107.5 to 116.4°, respectively, and similar corresponding numbers pertain for thioether-containing iron porphyrin complexes.[29c,d] There is a general (perhaps expected) trend in the thioether complexes that the larger C–S–C angles are associated with the smaller metal–S–C bond angles; complex **3**, however, has the largest C–S–C angle, 103.3°, as well as relatively large Ru–S–C angles (115.4, 110.9°), and suggests that nonbonding interactions between the two phenyl rings and between the phenyl and porphyrin rings may be significant.

Table VII. UV/Vis Spectral^a Data for Ruthenium(II) Octaethylporphyrin Complexes in Order of Increasing Wavelength of the Soret Band

	λ, nm			
complex^b	Soret	β	α	ref^c
Ru(PhNO)$_2$	392	505	531	60
Ru(NO)(OMe)	392	539	572	34
Ru(CO)(EtOH)	393	515	548	61
Ru(CO)	393	512	547	61
Ru(CO)(THF)	394	517	549	62
Ru(py)$_2$	395	495	521	34
Ru(CO)(Im)	396	518	550	63a
Ru(CO)(py)	396	518	549	34
Ru[P(*p*-MeOC$_6$H$_4$)$_3$]$_2$	396	505	533	41b
Ru(CO)(DecMS)	401	518	549	64
Ru(CO)(AsPh$_3$)	406	525	554	63b
Ru(CO)(PPh$_3$)	407	525	555	61
Ru(DecMS)$_2$	408	498	525	tw
Ru(SPh$_2$)$_2$	408	502	527	tw
Ru(DMSO)$_2$	~408	(515–540)^d		40b
Ru(CO)(P-*n*-Bu$_3$)	408	528	555	61
Ru(AsPh$_3$)$_2$	419	507	530	63b
Ru(PPh$_3$)$_2$	420	518	532	61
Ru(P-*n*-Bu$_3$)$_2$	428	511	535	61

[a] In C_6H_6 or CH_2Cl_2; the band positions are essentially solvent-independent. [b] *Ru* = Ru(OEP). [c] tw = this work. [d] Broad, unresolved band.

Other average bond lengths and angles for the metalloporphyrin moiety within **2** and **3** show no unusual features when compared with those of other monomeric, six-coordinate ruthenium porphyrin complexes (Table VI). The variable orientations found for the ethyl groups within OEP are not unusual and have been discussed previously, but not rationalized.[41b,58] The hydrocarbon tails with complex **2**, as they extend out in opposite directions from the porphyrin core, show no disorder problems, and the ^{1}H NMR signals of the bound DecMS are correspondingly completely resolved (see below).

Visible Absorption Spectra. The visible absorption spectra of the bis(thioether) complexes **2** and **3** are typical of six-coordinate, low-spin, ruthenium(II) porphyrin complexes (Table VII). Such spectra, dominated by the Soret (B) and α and β (Q) bands, have been considered in detail by the groups of Gouterman and Buchler.[34,59] In the spectra of complexes of the group 1–5 metals

---

(42) Pauling, L. *The Nature of the Chemical Bond* 3rd ed.; Cornell University Press: Ithaca, NY, 1960; pp 246, 250.

(43) March, F. C.; Ferguson, G. *Can. J. Chem.* **1971**, *49*, 3590.

(44) McMillan, R. S.; Mercer, A.; James, B. R.; Trotter, J. *J. Chem. Soc., Dalton Trans.* **1975**, 1006.

(45) Mercer, A.; Trotter J. *J. Chem. Soc., Dalton Trans* **1975**, 2480.

(46) Davies, A. R.; Einstein, F. W. B.; Farrell, N. P.; James, B. R.; McMillan, R. S. *Inorg. Chem.* **1978**, *17*, 1965.

(47) Killops, S. D.; Knox, S. A. R.; Riding, G. H.; Welch, A. J. *J. Chem. Soc., Chem. Commun.* **1978**, 486.

(48) Moody, D. C.; Ryan, R. R. *J. Chem. Soc., Chem. Commun.* **1980**, 1230.

(49) Gould, R. O.; Stephenson, T. A.; Thompson, M. A. *J. Chem. Soc., Dalton Trans.* **1980**, 804.

(50) Oliver, J. D.; Riley, D. P. *Inorg. Chem.* **1984**, *23*, 156.

(51) Kalinin, A. E.; Gusev, A. I.; Struchkov, Y. T. *J. Struct. Chem. (Engl. Transl.)* **1973**, *14*, 804.

(52) Coucouvanis, D. *Prog. Inorg. Chem.* **1979**, *26*, 301.

(53) Koch, S. A.; Millar, M. *J. Am. Chem. Soc.* **1983**, *105*, 3362.

(54) Bucknor, S. M.; Draganjac, M.; Rauchfuss, T. B.; Ruffing, C. J.; Fultz, W. C.; Rheingold, A. L. *J. Am. Chem. Soc.* **1984**, *106*, 5379.

(55) Draganjac, M.; Ruffing, C. J.; Rauchfuss, T. B. *Organometallics* **1985**, *4*, 1909.

(56) Little, R. G.; Ibers, J. A. *J. Am. Chem. Soc.* **1973**, *95*, 8583.

(57) Bonnet, J. J.; Eaton, S. S.; Eaton, G. R.; Holm, R. H.; Ibers, J. A. *J. Am. Chem. Soc.* **1973**, *95*, 2141.

(58) Thackray, D. C.; Ariel, S.; Leung, T. W.; Menon, K.; James, B. R.; Trotter, J. *Can. J. Chem.* **1986**, *64*, 2440.

(59) (a) Gouterman, M. In *The Porphyrins*; Dolphin, D., Ed.; Academic: New York, 1978; Vol. III, Chapter I. (b) Buchler, J. W. *Angew. Chem., Int. Ed. Engl.* **1978**, *17*, 407.

(60) Crotti, C.; Sishta, C.; Pacheco, A. P.; James, B. R. *Inorg. Chim. Acta* **1988**, *141*, 13.

(61) Barley, M.; Becker, J. Y.; Domazetis, G.; Dolphin, D.; James, B. R. *Can. J. Chem.* **1983**, *61*, 2389.

(62) Eaton, G. R.; Eaton, S. S. *J. Am. Chem. Soc.* **1975**, *97*, 235.

(63) (a) Barley, M.; Dolphin, D.; James, B. R.; Kirmaier, C.; Holten, D. *J. Am. Chem. Soc.* **1984**, *106*, 3937. (b) Barley, M.; Dolphin, D.; James, B. R. *J. Chem. Soc., Chem. Commun.* **1984**, 1499.

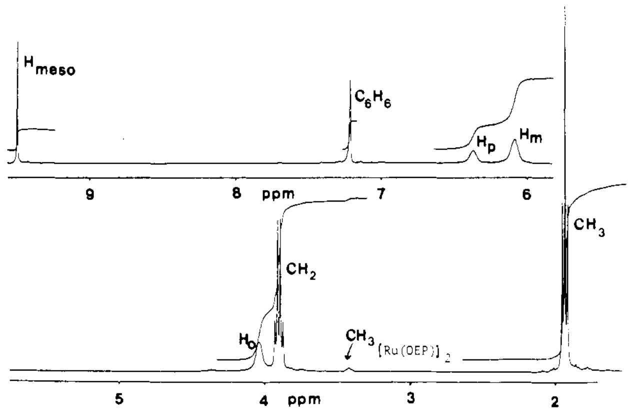

Figure 3. Room-temperature 400-MHz ^{1}H NMR spectrum of Ru(OEP)(SPh$_2$)$_2$ in C$_6$D$_6$.

in oxidation states I–V, respectively, the α band is seen in the 570–600-nm range; however, for a range of M(OEP)LL′ complexes (M = Ru, Os; axial ligands L, L′ = first-row donors such as CO and O- and N-donors), the α band is blue-shifted and an inverse correlation was established between the degree of metal → axial ligand π-bonding and the extent of the shift.[34]. The α bands of **2** and **3** (525 and 527 nm) are among the most hypsochromically shifted yet observed, and thus this suggests (as do the structural data) that π-back-bonding in these systems is weak. Our findings suggest that data for S-donor axial ligands fit the rule of bathochromism established earlier.[34,59] The positions of the α band of the tertiary phosphine systems (Table VII: in the 530-nm region for the bis(phosphine) complexes and in the 550-nm region for the carbonyl phosphine complexes) seem a reasonable measure of the axial ligand π-back-bonding.

A further, empirical trend seen in the data of Table VII is that within the Ru(OEP)LL′ complexes: where at least one axial ligand is a P-, As-, or S-donor *except* the tris(p-methoxyphenyl)phosphine species, the Soret band lies above 400 nm, while if L and L′ are first-row donors, the Soret band comes below 400 nm. Such a qualitative trend could prove useful when the axial ligands contain ambident, first- and later-row donor sites (e.g. sulfoxides, aminophosphines, etc). The data (Table VII) suggest that the briefly mentioned Ru(OEP)(DMSO)$_2$ complex[40a] contains at least one S-bonded DMSO ligand.

That excess Ph$_2$S is required for the room-temperature solution spectra of **3** to obey the Beer–Lambert law, over a concentration range of (1–5) × 10^{-4} M of the complex, implies that some dissociation of the axial thioether is occurring under such dilute conditions (cf. the quantitative analysis of a similar six-coordinate/five-coordinate equilibrium for Ru(OEP)(PPh$_3$)$_2$[41b]); the dissociation of the thioether ligands is discussed further in the section on ^{1}H NMR Spectra. The UV/vis spectral data for **2** reveal that no measurable dissociation of DecMS occurs over a similar concentration range.

^{1}H NMR Spectra. Figures 3 and 4a show the room-temperature ^{1}H NMR spectra of Ru(OEP)L$_2$, L = Ph$_2$S (**3**) and DecMS (**2**), while Figure 4b shows the corresponding spectrum of free DecMS. The broadness of some of the resonances in Figures 3 and 4a led us to study the temperature dependence of the spectra of **3** (Figure 5) and **2** (Figure 6).

The room-temperature spectra (Figures 3 and 4a and Experimental Section) are consistent with the solid-state structures. The porphyrin ring resonances (H$_{meso}$, –CH$_2$–, –CH$_3$) are typical of those for diamagnetic species containing OEP,[35,41b] while the equivalence of the methylene protons of the ethyl groups demonstrates mirror symmetry in the porphyrin plane for the solution structures.[35] The upfield phenyl resonances of the coordinated Ph$_2$S result from the ring current effect exerted by the porphyrin, and the shifts for the ortho, meta, and para protons are similar to those observed for the corresponding bis(triphenylphosphine) complex.[41b] A corresponding feature of the spectrum of the coordinated DecMS ligand is the complete resolution of the methylene and methyl protons; similar shifts have been reported for Rh(OEP)R complexes, where R = n-hexyl and n-nonyl,[65] but the extent to which the signals of bound DecMS are spread out relative to those of the free ligand (Figure 4b) illustrates the potential use of metalloporphyrins as "derivatizing reagents" for ligands with unresolved ^{1}H NMR spectra.[66]

The temperature dependences of the NMR spectra are informative. The room-temperature broad phenyl proton signals of coordinated Ph$_2$S in **3** sharpen at 0 °C into two well-defined triplets and a doublet, while the porphyrin peaks are sharp at both temperatures (Figures 3 and 5); further, at 0 °C, two multiplets appear at δ ~6.9 and ~7.2, which correspond to those we measured for free Ph$_2$S. As the temperature is raised to 65 °C (Figure 5), the axial ligand peaks broaden and shift downfield toward the free Ph$_2$S positions, while the δ 6.9 and 7.2 multiplets coalesce into a hump that initially lies under the C$_7$H$_8$ (solvent) peaks at ~7 ppm but then moves somewhat upfield; at 65 °C, all three peaks of bound Ph$_2$S have coalesced with each other and the broad hump to give a time-averaged resonance at 6.65 ppm. Correspondingly, as one goes from 0 to 65 °C, a small peak at 3.5 ppm shifts to ~3.2 ppm and becomes more prominent and three other peaks become evident at ~23, 10.3, and 9.7 ppm; these four peaks are assigned to the paramagnetic species [Ru(OEP)]$_2$, a drastically shifted methylene proton at 20+ ppm being particularly diagnostic.[35] Finally, even at 65 °C the porphyrin proton signals from [Ru(OEP)]$_2$ and Ru(OEP)(SPh$_2$)$_2$ remain separate, showing that ligand exchange between these species is slow.

The above NMR data for **3** can be rationalized in terms of the equilibria outlined in reactions 5 and 6. The latter is written as

$$\underset{\mathbf{3}}{\mathrm{Ru(OEP)(SPh_2)_2}} \underset{k_{-1}}{\overset{k_1}{\rightleftharpoons}} \mathrm{Ru(OEP)(SPh_2)} + \mathrm{Ph_2S} \qquad (5)$$

$$\mathrm{Ru(OEP)(SPh_2)} \underset{k_{-2}}{\overset{k_2}{\rightleftharpoons}} {}^1/_2[\mathrm{Ru(OEP)}]_2 + \mathrm{Ph_2S} \qquad (6)$$

a single step showing direct formation of the dimer, although this will almost certainly proceed via an intermediate "Ru(OEP)" species,[6] which presumably rapidly dimerizes. At room temperature, the combined equilibria must incorporate exchange between **3** and the dimer that is too slow to generate significant line broadening, because the individual OEP resonances for these two species are sharp; the observed line broadening of the coordinated Ph$_2$S must result from k_1 and k_{-1} being much larger than k_2 and k_{-2}. The overall K_1 value (k_1/k_{-1}), however, must be very small for this labile equilibrium—the porphyrin protons must spend most of their time as Ru(OEP)(SPh$_2$)$_2$. The K_2 equilibrium (reaction 6) provides a pool of free Ph$_2$S ligand with which **3** can exchange and accounts for the observed broadening of the signals due to bound and free Ph$_2$S. As the temperature increases, the combined equilibria K_1K_2 (and almost certainly the individual K_1 and K_2 values) increase, and more dimer is formed, although exchange of this with **3** clearly remains slow; at the same time, k_1 and k_{-1} increase to the point where rapid exchange occurs between coordinated and free Ph$_2$S, while the ever-increasing pool of free Ph$_2$S results in a time-averaged peak for the Ph$_2$S protons that moves closer to the free ligand positions. When the NMR sample tube was subsequently cooled, the K_1K_2 equilibria did slowly shift to the left, as evidenced visibly by a color change from the brownish solution of the dimer to the red complex **3** over a period of 1–2 days. The conversion of dimer to **3** constitutes, of course, the basis of the synthesis used for **3**, and the slowness of the reaction under NMR conditions explains why in the synthetic procedure described in the Experimental Section it was necessary to concentrate the solution to give effective conversion. That the

---

(64) Pacheco, A.; James, B. R., to be submitted for publication. The species is readily prepared in situ by treating a benzene solution of **2** with 1 atm of CO.

(65) Ogoshi, H.; Setsune, J.; Omura, T.; Yoshida, Z. *J. Am. Chem. Soc.* **1975**, *97*, 6461.

(66) Choy, C. K.; Mooney, R. J.; Kenney, M. E. *J. Magn. Reson.* **1979**, *35*, 1.

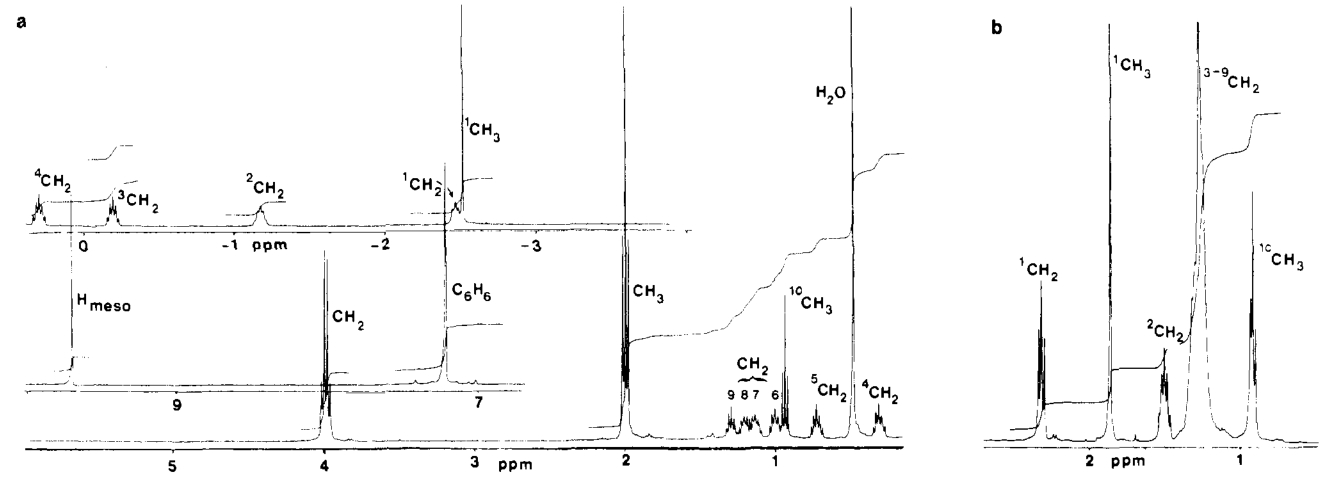

Figure 4. Room-temperature 400-MHz ^1H NMR spectra of (a) $Ru(OEP)(DecMS)_2$ and (b) free DecMS in C_6D_6.

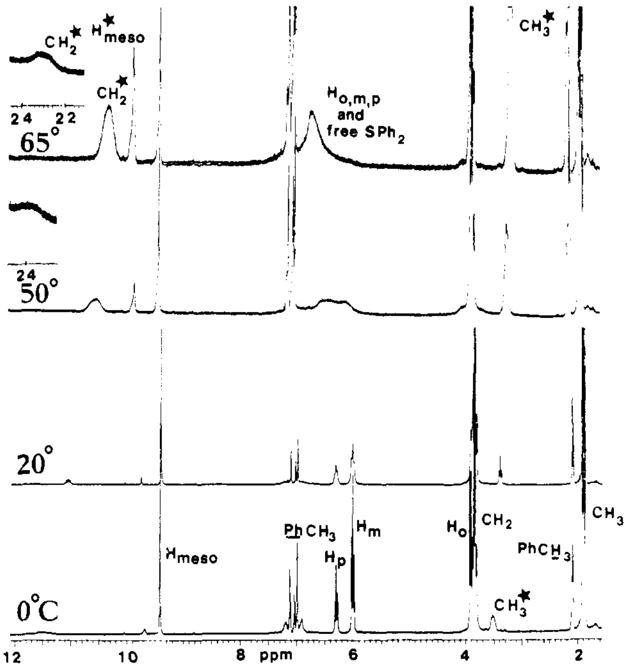

Figure 5. Temperature-dependent ^1H NMR spectrum (300 MHz) of $Ru(OEP)(SPh_2)_2$ in toluene-d_8 at 0, 20, 50, and 65 °C. Resonances labeled with an asterisk (*) are attributed to $[Ru(OEP)]_2$.

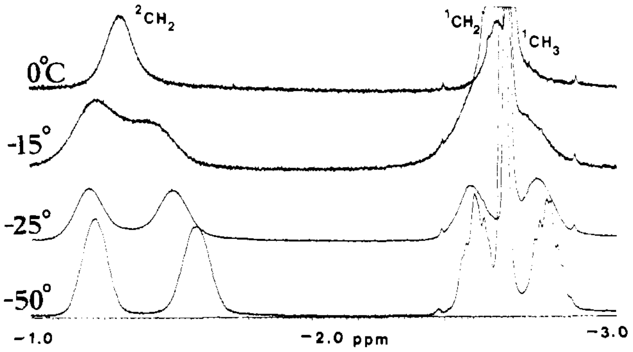

Figure 6. Temperature-dependent ^1H NMR spectrum (300 MHz) of $Ru(OEP)(DecMS)_2$ in toluene-d_8, -1.0, to -3.0 ppm region.

^1H NMR signals of the $[Ru(OEP)]_2$ component are essentially the same at room temperature and at 0 °C implies that the dimer and free Ph_2S are kinetically trapped at the lower temperatures.

Although no NMR evidence was found for the five-coordinate intermediate at the 10^{-3}–10^{-2} M concentrations of **3** used, the UV/vis data at more dilute concentrations (see above), where the equilibria of reactions 5 and 6 would be favored, offer support for dissociation of some kind. Attempts to study quantitatively the dissociation by UV/vis spectra were thwarted by the extreme air sensitivity of the necessarily very dilute solutions; qualitatively, on consideration of the NMR data, about 10% of complex **3** has dissociated into dimer and Ph_2S at 20 °C.

The room-temperature ^1H NMR spectrum of **2** does not show any obvious abnormal broadening of the DecMS signals compared to those of the OEP moiety; however, cooling of the sample reveals first broadening of the δ -2.46 (S–$^1CH_2$) and -1.17 (–S–C-H_2–$^2CH_2$) resonances, and then, below -20 °C, these signals split into two equal-intensity peaks (Figure 6), showing that the methylene protons on both ^1C and ^2C are now detectably inequivalent. This must result from the prochiral nature of the thioether; on coordination of sulfur, this atom becomes chiral and the pairs of protons on the associated carbon atoms become diastereotopic and hence anisochronous.[67,68] All the other signals in the ^1H NMR spectrum broadened to some extent at the lower temperatures, but no further splitting was observed. Clearly, at room temperature, a fast exchange process is giving rise to an averaged signal for the diastereotopic CH_2 protons; possible mechanisms include[67,68] (a) an intramolecular pyramidal inversion at the sulfur, where possible transition states include structures governed by bonding to both sulfur lone pairs, or at least both lobes of a p orbital and (b) dissociaton of a thioether ligand and reattachment via the other lone pair. The former mechanism has been demonstrated within four-coordinate Pt(II) and Pd(II) complexes[68b] and is strongly favored for six-coordinate Rh(III) and Ir(III) systems,[68a] the energy barriers of inversion being in the 50–80 kJ mol^{-1} range. Such a process seems plausible for our porphyrin system and, somewhat analogous to the required transition state, seven-coordinate ruthenium porphyrins have been suggested;[69] qualitatively, the NMR data for **2** would imply a relatively low value for the inversion barrier. A ^1H NMR spectrum of solutions of **2** containing excess DecMS at room temperature was simply an addition of the two components, thus showing no evidence for ligand exchange, which argues strongly against mechanism b.[70] The behavior of **2** contrasts with that

---

(67) Abel, E. W.; Farrow, G. W.; Orrell, K. G. *J. Chem. Soc., Dalton Trans.* **1976**, 1160.

(68) (a) Abel, E. W.; Farrow, G. W.; Orrell, K. G.; Sik, V. *J. Chem. Soc., Dalton Trans.* **1977**, 42. (b) Abel, E. W.; Ahmed, A. K. S.; Farrow, G. W.; Orrell, K. G.; Sik, V. *J. Chem. Soc., Dalton Trans.* **1977**, 47.

(69) Domazetis, G.; James, B. R.; Dolphin, D. *Inorg. Chim. Acta* **1981**, *54*, L47.

(70) This ^1H NMR experiment also rules out exchange via an associative process. Such a mechanism (or an interchange mechanism[71]) for substitution at the Ru in these thioether systems may be operative in some cases; thus, in situ formation[64] of Ru(OEP)(CO)(DecMS) (Table VII) is rapid, although thioether exchange is slow. Detailed kinetic studies on these substitution processes are in progress.

(71) Wilkins, R. G. *The Study of Kinetics and Mechanism of Reactions of Transition Metal Complexes*; Allyn and Bacon: Boston, MA, 1974; p 187.

of **3**, where thioether exchange with the less basic, and more weakly coordinated, Ph_2S was observed. For **2** to obey the Beer–Lambert law even in dilute solutions ($\sim 10^{-4}$ M), it is required that any dissociation to a five-coordinate species be negligible (certainly nondetectable).

Worthy of note is that both S atoms within $Ru(OEP)(DecMS)_2$ are chiral, of course, while the crystal structure contains only the *R,S* diastereomer (the meso compound). The ^1H NMR spectra have been rationalized in terms of the presence of a single diastereomer (e.g. *R,S*) with rapid interconversion at the S atoms at ambient conditions (e.g. to the *S,R* form). Chemically, we see no reason why the *R,R* and *S,S* forms are not equally viable, and the solution could contain the three diastereomers, *meso*, *R,R*, and *S,S*, in the ratios 2:1:1, the forms being indistinguishable by ^1H NMR methods.

A final observation is that the positions of all of the ^1H NMR signals of **2** are temperature-dependent. Small, regular shifts on the order of 0.02–0.04 ppm (in either direction) over a 65 °C range are common in diamagnetic metalloporphyrins, for both the porphyrin and the axial ligand protons.[72] In $Ru(OEP)(DecMS)_2$, however, the shifts for the methylene protons on ^1C to ^4C are more substantial (0.07–0.14 ppm); for both $^1CH_2$ and $^2CH_2$, the averaged signal (either measured as such above 0 °C or estimated from the split signals observed below −25 °C) moves downfield with increasing temperature from −50 to +15 °C, and the data, measured in toluene on the 300-MHz machine, strictly follow the empirical linear relationships $\delta_{^1CH_2} = -2.99 + 0.0014T$ and $\delta_{^2CH_2} = -1.905 + 0.0023T$ (the temperature T is given on the Kelvin scale). Surprisingly, the signal of the S–CH_3 protons shifts downfield only 0.015 ppm over the same −50 to +15 °C range.

Preliminary Oxidation Studies. A few experiments have been carried out to explore the reactivity of complexes **2** and **3** toward O_2/air[73] in both the presence and the absence of the respective thioether. Benzene solutions of the bis(diphenyl sulfide) complex **3** at room temperature are extremely air-sensitive with or without added Ph_2S, but neither sulfoxide nor sulfone was produced; the thioether, including that originally coordinated, is recoverable while the metal is converted to the known Ru(IV)–μ-oxo species $[(HO)Ru(OEP)]_2O$.[7,74] Some recent findings reveal a propensity for five-coordinate ruthenium(II) porphyrin complexes[17] (and $[Ru(OEP)]_2$,[75] also five-coordinate) to undergo readily this oxidation to the μ-oxo species, and indeed consideration of the UV/vis and ^1H NMR data for **3** has shown the importance of $Ru(OEP)(SPh_2)$ and $[Ru(OEP)]_2$ intermediates. For the more basic DecMS system, it was not necessary to invoke such five-coordinate species to explain the spectral data and, perhaps in line with this, **2** is not particularly air-sensitive in dry solvents and does not generate the μ-oxo species. In the presence of excess decyl methyl sulfide, **2** does catalyze a very slow autoxidation of the thioether, and the reaction is accelerated if the solutions are made acidic. For example, in a 10^{-3} M benzene solution of **2**, containing 1.5×10^{-4} M acetic acid and 0.1 M DecMS and being left in air for 3 days at ambient conditions, about half of the thioether is converted to the sulfoxide; some other, as yet unidentified, organosulfur products are also present (in the absence of **2** the oxidation rate is negligible). Further, the selectivity for sulfoxide formation varies with acid concentration, water content, and temperature. The formation of sulfoxide could be accommodated by the mechanism outlined in reactions 1–4, on replacing PPh_3 by DecMS. Kinetic and mechanistic studies are in progress in attempts to elucidate the reaction pathway(s) in these thioether oxidations.

Acknowledgment. We thank the Natural Sciences and Engineering Research Council of Canada (B.R.J.) and the U.S. National Institutes of Health (Grant HL 13157 to J.A.I.) granting agencies for financial support, Johnson Matthey Ltd. for the loan of Ru, and Professor J. Trotter for use of crystallographic facilities.

Registry No. 1, 54762-43-5; 2, 114597-20-5; 3, 114597-21-6; DecMS, 22438-39-7; S, 7704-34-9.

Supplementary Material Available: Listings of calculated hydrogen parameters, all bond lengths and angles, anisotropic thermal parameters, displacements of atoms from the porphyrin plane, and dihedral angles between the porphyrin core and pyrrole rings for $Ru(OEP)L_2$, L = DecMS and Ph_2S (9 pages); listings of observed and calculated structure amplitudes (65 pages). Ordering information is given on any current masthead page.

---

(72) Janson, T. R.; Katz, J. In *The Porphyrins*; Dolphin, D., Ed.; Academic: New York, 1979; Vol. VI, Chapter I.

(73) We have found previously[8] that air provides an effective O_2 plus H^+ reagent for oxidation of Ru(II) to Ru(III) (cf. eq 1 and 2).

(74) Masuda, H.; Taga, T.; Osaki, K.; Sugimoto, H.; Mori, M.; Ogoshi, H. *J. Am. Chem. Soc.* **1981**, *103*, 2199.

(75) Collman, J. P.; Barnes, C. E.; Collins, T. J.; Brothers, P. J.; Gallucci, J.; Ibers, J. A. *J. Am. Chem. Soc.* **1981**, *103*, 7030.